This is an open access article published under a Creative Commons Attribution (CC-BY) License, which permits unrestricted use, distribution and reproduction in any medium, provided the author and source are cited.

LANGMUIR

Article

pubs.acs.org/Langmuir

Nonequilibrium Molecular Dynamics Simulations of Organic Friction Modifiers Adsorbed on Iron Oxide Surfaces

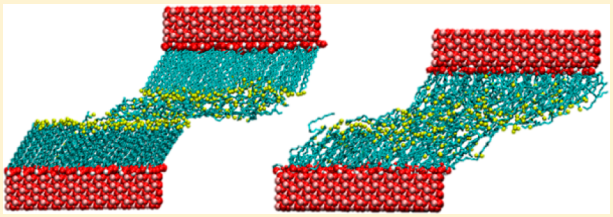
James P. Ewen,*[,†] Chiara Gattinoni,[†] Neal Morgan,[‡] Hugh A. Spikes,[†] and Daniele Dini[†]

[†]Department of Mechanical Engineering, Imperial College London, London SW7 2AZ, England

[‡]Shell Global Solutions UK Ltd, Manchester M22 0RR, Lancashire, England

Supporting Information

ABSTRACT: For the successful development and application of lubricants, a full understanding of the nanoscale behavior of complex tribological systems is required, but this is difficult to obtain experimentally. In this study, we use nonequilibrium molecular dynamics (NEMD) simulations to examine the atomistic structure and friction properties of commercially relevant organic friction modifier (OFM) monolayers adsorbed on iron oxide surfaces and lubricated by a thin, separating layer of hexadecane. Specifically, acid, amide, and glyceride OFMs, with saturated and Z-unsaturated hydrocarbon tail groups, are simulated at various surface coverages and sliding velocities. At low and medium coverage, the OFMs form liquidlike and amorphous monolayers, respectively, which are significantly interdigitated with the hexadecane lubricant, resulting in relatively high friction coefficients. At high coverage, solidlike monolayers are formed for all of the OFMs, which, during sliding, results in slip planes between well-defined OFM and hexadecane layers, yielding a marked reduction in the friction coefficient. When present at equal surface coverage, OFMs with saturated and Z-unsaturated tail groups are found to yield similar structure and friction behavior. OFMs with glyceride head groups yield significantly lower friction coefficients than amide and particularly carboxylic acid head groups. For all of the OFMs and coverages simulated, the friction coefficient is found to increase linearly with the logarithm of sliding velocity; however, the gradient of this increase depends on the coverage. The structure and friction details obtained from these simulations agree well with experimental results and also shed light on the relative tribological performance of these OFMs through nanoscale structural variations. This has important implications in terms of the applicability of NEMD to aid the development of new formulations to control friction.



INTRODUCTION

In order to reduce energy consumption and thus CO_2 emissions, it is necessary to increase the energy efficiency of engineering systems and an important way to achieve this is to design lubricants that give low friction. This need for greater energy efficiency has led to a shift toward lower-viscosity lubricants, which means that an increasing number of engineering components operate under boundary (thin film) lubrication conditions. As a result, lubricant additives that reduce friction and wear under boundary conditions are of increasing importance.[1] Moreover, with growing concern that engine exhaust after-treatment systems may be poisoned by elements found in some types of friction modifier additives,[2] there has been a resurgence of interest in organic friction modifier (OFM) additives which are based solely on C, H, O, and N atoms.

OFMs are amphiphilic surfactant molecules that contain a nonpolar hydrocarbon tail group attached to a polar head group.[3] The generally accepted friction reduction mechanism involves the adsorption of the polar head group to metal or ceramic surfaces, with strong, cumulative van der Waals forces between proximal nonpolar tails leading to the formation of incompressible monolayers that prevent contact between solid surfaces to reduce adhesion and friction.[4]

Many different amphiphiles have been tested as OFMs, and there are three main structural variables: (i) the nature of the head group, (ii) the length of the hydrocarbon tail, and (iii) the structure of the hydrocarbon tail, whether straight or branched and whether saturated or unsaturated.[1] Early OFMs contained carboxylic acid head groups; however, these were soon found to cause high levels of corrosion for some bearing metals, and they were gradually replaced in most applications by less corrosive amphiphiles such as amines, amides, esters, or chelating combinations of such groups.[1] Nonetheless, most experimental[3−13] and simulation[14−19] tribology studies have utilized OFMs with carboxylic acid head groups. There have been far fewer studies of the more commercially relevant amine,[20−22] amide,[9,23] or glyceride[2,10] OFMs. Boundary friction experiments have shown that glyceride[10] and amide[9] OFMs can yield lower friction coefficients than their acid counterparts, though the reasons for this were yet to be established prior to this current study. With respect to tail group selection, commercial OFMs generally utilize unbranched aliphatic tail groups containing 12−20 carbon atoms as a result of their effective

Received: February 15, 2016
Revised: April 5, 2016

 © XXXX American Chemical Society

DOI: 10.1021/acs.langmuir.6b00586
Langmuir XXXX, XXX, XXX−XXX

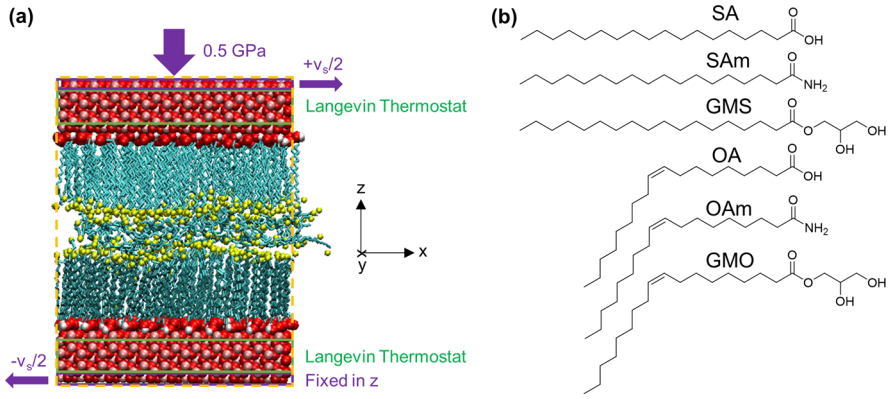


Figure 1. Simulation details: setup for compression and sliding simulations (a). Example shown for SA at high coverage after compression, before sliding. Head groups are shown with O in red and H in white, terminal C in yellow, and the other tail group C in cyan. Hydrogen atoms in the tail groups are omitted for clarity. In the slab, Fe atoms are shown in pink. Periodic boundary conditions (yellow dotted line) are applied in the *x* and *y* directions. Rendered using VMD.[45] Chemical structures of OFMs simulated in this study (b): stearic acid (SA), stearic amide (SAm), glycerol monostearate (GMS), oleic acid (OA), oleamide (OAm), and glycerol monooleate (GMO).

friction reduction,[6] high base oil solubility, and availability from natural fats and oils.[1] These natural fats and oils contain mixtures of molecules with saturated as well as mono and polyunsaturated tail groups which are generally used collectively rather than being separated into individual tail group types.[1] The most widely studied components in the literature are saturated C_{18} chains (stearyl) and monounsaturated C_{18} chains with an unsaturated Z-alkene at the C_9 position (oleyl).[1] Boundary friction experiments at equal concentration showed that OFMs with saturated tails, such as stearic acid and glycerol monostearate, gave low friction coefficients which increased linearly with the logarithm of sliding velocity.[10] Conversely, OFMs with Z-unsaturated tails, such as oleic acid and glycerol monooleate, yielded significantly higher friction coefficients that remained relatively constant with sliding velocity.[10] One aspect of this current study is to establish whether these observations are due to differences in the nanoscale structure of the film or simply arise from a lower surface coverage at a given concentration as a result of the "kinks" from the Z-alkene in the middle of the tail group.

In order to understand how the head and tail groups influence the performance of OFMs, it is necessary to obtain a clear picture of (i) the structure of the OFM film and its modification of the interface between the polar metal oxide surface and the hydrocarbon lubricant and (ii) the effect that this has on the friction coefficient. Detailed structural information on OFM films at the surface−lubricant interface can be obtained from experimental techniques such as sum frequency spectroscopy (SFS),[23] polarized neutron reflectometry (PNR),[11,20] the surface force apparatus (SFA),[8] and in situ atomic force microscopy (AFM).[13,22] These methods can be used to monitor monolayer formation and gather information such as the OFM film thickness and tilt angle. The friction behavior of OFM films can also be investigated using AFM[13,22] and SFA[8] as well as dedicated boundary friction experiments.[9,10] The experimental boundary friction results discussed in this study come mainly from sliding tests using a steel−steel, ball-on-disk contact and a hexadecane solvent.[10] These tests employ low sliding velocities (mm s^{-1}) and high pressures (GPa) in order to minimize lubricant entrainment and thus maintain boundary lubrication conditions.

Classical molecular dynamics simulations can be used to simultaneously probe the nanoscale structure and friction of OFM films,[16,21] making it a valuable complement to experiments. The use of well-tested all-atom force fields yields an accurate representation of the structure of large systems (tens of thousands of atoms), where the collective behavior of many OFM molecules can be reliably analyzed over time. Moreover, nonequilibrium molecular dynamics (NEMD) simulations can provide important information on the frictional behavior of the system under a range of conditions. Indeed, NEMD simulations have provided unique insights into the friction behavior of a multitude of systems, from alkylsilane monolayers on silica surfaces[24] to diamondlike carbon (DLC) coatings[25] and platinum AFM tips on gold surfaces.[26] Previous NEMD simulations of OFM monolayers have analyzed the film structure and friction of acid[16] and amine[21] OFMs using reasonably thick lubricant films, low pressure (P_z = 0.1 GPa), and relatively low coverages. NEMD simulations have also been used to quantify the Derjaguin offset in high-coverage carboxylic acid films both in intimate contact and separated by a thin layer of lubricant.[15] It has been suggested from these simulations that OFM monolayers that are less interdigitated[16] and smoother[15] yield lower friction coefficients. However, the specifics of how the OFM film structure and friction change with molecular structure, coverage, and sliding velocity are yet to be fully explored in systems with thin lubricant films under high pressure (P_z = 0.5 GPa) as used in boundary friction experiments.[10]

Thus, the aim of the current study is to use NEMD simulations to shed light on the nanoscale structure of OFM films adsorbed on iron oxide surfaces and separated by a thin layer of hexadecane to calculate the friction coefficient as a function of coverage and sliding velocity and to fully explore links between the structure and friction. A wide range of OFMs are explored in order to better understand the influence of head group type and tail group Z-unsaturation on structure and friction (Figure 1b). In addition, the use of OFM films with a wide range of coverages, including close to the theoretical limit, should indicate the significance of the formation of close-packed monolayer films in the reduction of boundary friction. The velocity dependence of the friction coefficient for different OFMs and coverages will also be analyzed and compared to boundary friction experiments. The structure of the remainder of this publication will now be outlined. First, the general system setup for all of the simulations is introduced, followed

DOI: 10.1021/acs.langmuir.6b00586
Langmuir XXXX, XXX, XXX−XXX

by the specific methodology for the preliminary squeeze-out and compression and sliding simulations. This is followed by the results of the preliminary squeeze-out simulations and finally the structure and friction results from the compression and sliding simulations are discussed in detail.

METHODOLOGY

System Setup. A representative example of the systems simulated in this study is shown in Figure 1a. It consists of a thin layer of hexadecane lubricant confined between two OFM monolayers adsorbed on iron oxide slabs. All structures were constructed using the Materials and Processes Simulations Platform (MAPS) from Scienomics SARL. Three different OFM head groups (carboxylic acid, amide, and glyceride) and two different tail groups (stearyl and oleyl) are considered in these simulations. Acid OFMs were selected to allow comparison to previous experiments and simulations, whereas amide and glyceride OFMs are more commercially relevant.[1] Specifically, NEMD simulations were used to compare the structure and friction of stearic acid (SA), oleic acid (OA), stearic amide (SAm), oleamide (OAm), glycerol monostearate (GMS), and glycerol monooleate (GMO) films over a range of surface coverages and sliding velocities (Figure 1b). Hexadecane was chosen as a model base oil because its properties are well-defined, and it is commonly employed in both experimental[10,13,22] and modeling[15,16,21] tribology studies. Given that charge separation is unfavorable in the low-polarity hexadecane solvent, all OFM molecules were assumed to be in their electronically neutral form.

Classical MD simulations were performed using LAMMPS.[27] In all of the MD simulations, (100) slabs of α-iron(III) oxide[28] (hematite) with dimensions (xyz) of approximately 55 Å × 55 Å × 12 Å were used as the substrates, representing a single asperity contact. Periodic boundary conditions were applied in the x and y directions. Care was taken to cleave the surface in a manner such that the Fe/O ratio remained at 2:3 in order to ensure that surfaces with no overall charge were produced. OFM molecules were oriented perpendicular to, and initially 3 Å from, the interior surfaces of two such slabs (Figure 1a). This produced OFM films similar to those formed by the Langmuir−Blodgett experimental procedure, e.g., ref 5. Hexadecane molecules were then randomly distributed between the OFM films.

If one assumes a monodentate binding mode for the glycerides, then the limiting head group area for all of the OFMs is around 22 Å^2.[29] The surface coverage or packing density can be quantified as the number of head groups per area of surface, Γ. A high surface coverage (Γ = 4.32 nm^{-2}), close to the maximum theoretical value,[29] is simulated by adsorbing 132 OFM molecules on each 3000 Å^2 slab to form a close-packed monolayer. Two other surface coverages are considered: a medium coverage (Γ = 2.88 nm^{-2}), which is approximately two-thirds of the maximum coverage, and a low coverage (Γ = 1.44 nm^{-2}), which is around one-third of the maximum coverage. The high-coverage simulation has been achieved experimentally on steel surfaces for acids and amides[29] but has not been reported for glycerides. However, previous MD simulations[2] as well as experimental results at the air−water interface[30] suggest that the high coverage employed should also be possible for glycerides. In tribology experiments, the OFM concentration in the lubricant is generally used rather than surface coverage because it is far easier to measure and control. PNR experiments of palmitic acid[11] suggest that at intermediate concentrations (150−1000 ppm) the surface coverage increases linearly with OFM concentration in the lubricant. However, in order to directly compare the OFM concentration and coverage, more research is required to understand the asymptotic behavior of the coverage at lower and higher concentrations for the specific molecules studied here.

A combination of several updated versions of the OPLS all-atom force field[31] were used to represent both hexadecane and the OFM molecules; full details and original references can be found in the Supporting Information. The OPLS family of force fields was chosen for three main reasons: (i) the inclusion of specific parameters for all of the functional groups required,[31,32] (ii) the all-atom representation that is expected to be critical in accurately modeling friction in this system (quantitative comparisons to be published separately), and (iii) recent parametrizations available which allow far more accurate representations of long-chain hydrocarbon than previously possible.[33] The final point is critical because the original OPLS parametrization has been shown to misrepresent the liquid−solid phase behavior of long-chain alkanes,[33,34] an issue which would certainly impact the behavior observed in these simulations. Lennard-Jones interactions were cut off at 10 Å,[34] and "unlike" interactions were evaluated using the geometric mean mixing rules, as prescribed in the OPLS force field.[31] Electrostatic interactions were not cut off but rather evaluated using a slab implementation of the PPPM algorithm.[35]

Surface−lubricant and surface−OFM interactions were represented by the Lennard-Jones and Coulomb potentials; the hematite surface parameters selected were developed by Berro et al.,[36] which are outlined in the Supporting Information. DFT calculations are also being conducted to better understand the nature and strength of the surface−OFM interactions. The hematite slab atoms were restrained in the corundum crystal by harmonic bonds between atoms within 3 Å. The force constant of these bonds was chosen to be 130 kcal mol^{-1} Å^{-2}, which has been shown previously to keep the surface structure suitably rigid but not to adversely affect the thermostatting.[36] It is worth noting that in previous MD simulations of the adsorption of similar molecules onto hematite surfaces the adsorption energy was dominated by the long-range electrostatic contribution between the head group and the polar surface.[14]

The MD equations of motion were integrated using the velocity Verlet algorithm with an integration time step of 1.0 fs. Fast-moving bonds involving hydrogen atoms were constrained with the SHAKE algorithm.[37] The Langevin thermostat,[38] with a time relaxation constant of 0.1 ps, was used in all of the simulations in order to maintain a temperature, T = 300 K. The pressure (P_z = 0.5 GPa) was controlled by applying a constant normal force to the outermost layer of atoms in the upper slab, keeping the z coordinates of the outermost layer of atoms in the lower slab fixed, as previously proposed[16,39] (Figure 1a).

Preliminary Squeeze-Out Simulations. To estimate the thickness of the central hexadecane film under the applied pressure, preliminary squeeze-out simulations were performed prior to the compression and sliding simulations. Previous simulations[40,41] and AFM experiments[42] of hydrocarbon squeeze-out between solid surfaces showed that there was an energy barrier to overcome when removing sufficient fluid to result in one fewer molecular layer. The size of this barrier increased when longer chains with a higher viscosity were used and also increased progressively when fewer molecular layers

DOI: 10.1021/acs.langmuir.6b00586
Langmuir XXXX, XXX, XXX−XXX

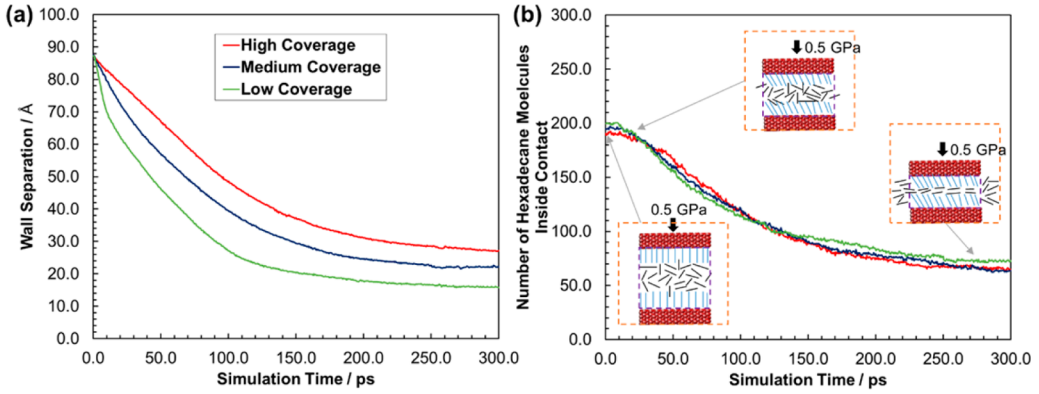


Figure 2. Results of squeeze-out simulations for representative OFM (SA) at different coverages: variation in the slab separation (a) and the number of hexadecane molecules within the contact volume (b), over 300 ps, P_z = 0.5 GPa. Inset schematics in (b) show the structure of the initial system, followed by compression of the OFM film and the squeeze out of hexadecane. Blue lines represent OFM molecules, and black lines represent hexadecane. The orange dotted line shows periodic boundaries, and the purple dotted line shows the contact volume.

remained in the contact.[40−42] Hence, a relatively large pressure was required to squeeze out the last few molecular layers of fluid. From these previous results, it was expected that an equilibrium thickness of between 1 and 3 molecular layers of hexadecane would remain in the contact under the simulation conditions (P_z = 0.5 GPa, T = 300 K).

Starting from the system described above, 50 Å of vacuum was added in the x and y directions to allow hexadecane molecules to be squeezed out of the contact, and the strongly adsorbed OFM molecules remained on the surface. Periodic boundary conditions were maintained outside of this extended system. At this stage, the thermostat was applied to the entire system. Hexadecane molecules (200) were randomly distributed between the OFM-covered slabs, corresponding to roughly 5 molecular layers for this contact area (~3000 Å^2). The slabs were moved closer together by applying a velocity (10 m s^{-1}) to the top slab until the density of the OFM and hexadecane region was similar to that of liquid hexadecane (0.75 g cm^{-3}) and the system was then energy-minimized. Pressure (P_z = 0.5 GPa) was then applied until the average slab separation reached equilibrium, after approximately 250 ps (Figure 2a). The number of hexadecane molecules remaining in the contact was estimated by dividing the number of hexadecane carbon atoms between the slabs by 16. This residual number of hexadecane molecules was used for the following compression and sliding simulations.

The addition of vacuum to the edge of the system may mean that so-called finite-size effects[43] influence the residual number of hexadecane molecules. Therefore, squeeze-out simulations were also conducted with system sizes two and four times as large as those used in the compression and sliding simulations to ensure consistency. Indeed, the squeeze-out data presented in the results and discussion section scaled well with system size, with the same number of hexadecane layers remaining inside the contact in the larger systems (Supporting Information).

Compression and Sliding Simulations. The compression and sliding simulations used systems containing a residual number of hexadecane molecules from the squeeze-out simulations, with the same three coverages of OFM molecules as outlined previously but with the vacuum in the x and y directions removed. A density similar to that of liquid hexadecane (0.75 g cm^{-3}) was reached by moving the top slab down at 10 m s^{-1} prior to energy minimization. The system was then pressurized (P_z = 0.5 GPa), thermostated in directions perpendicular to the compression (x and y), and allowed to equilibrate at 300 K. Initially, the slab separation varied in a damped harmonic manner, so sliding was not applied until a constant average slab separation was obtained and the hydrostatic pressure within the hexadecane film was close to its target value.[36] These compression simulations were generally around 200 ps in duration. During the compression stage, there was a collective tilting of the OFM molecules toward the surface in a random direction. The sliding direction (x) was chosen to be perpendicular to the orientation of this initial tilt (y). Previous NEMD simulations of monolayers in intimate contact, with the tilt orientated parallel to the sliding direction (x), have shown high friction and stick−slip behavior due to the high commensurability of the interface.[15,44] However, the presence of a thin, separating layer of hexadecane in previous NEMD simulations has been shown to maintain low friction.[15] Hence, the consistently low friction observed in boundary friction experiments[10] is expected to be reproduced in these simulations due to the presence of the hexadecane layer between the OFM films. Additional simulations with the sliding direction completely aligned with the initial tilt were also conducted to confirm that the initial orientation of the tilt did not influence the friction results obtained.

After compressive oscillation became negligible, a velocity of $v_x = \pm v_s/2$ was added in the x direction to the outermost layer of atoms in each slab (Figure 1a), and sliding simulations were conducted for 0.5−10 ns, depending on the sliding velocity, v_s. The values of v_s applied were 1, 2, 5, 10, and 20 m s^{-1}, and all simulations were run for long enough to yield a sufficient sliding distance (10 nm) to obtain representative values for the friction coefficients (uncertainty <10%). Although lower sliding velocities are desirable to match those used in boundary friction experiments (typically mm s^{-1}), they are not yet accessible using all-atom NEMD simulations on this scale.[16] During the sliding simulations, any heat generated was dissipated using a thermostat acting only on the middle 10 Å of both iron oxide slabs (Figure 1a), applied in the direction perpendicular to the both the sliding and compression (y).[46] This is known to be advantageous over direct thermostatting of the fluid, which has been shown to significantly affect the behavior of confined fluids under sliding conditions.[47] The boundary thermostatting method applied here has been shown previously to be effective in controlling the temperature of similar systems and sliding

DOI: 10.1021/acs.langmuir.6b00586
Langmuir XXXX, XXX, XXX−XXX

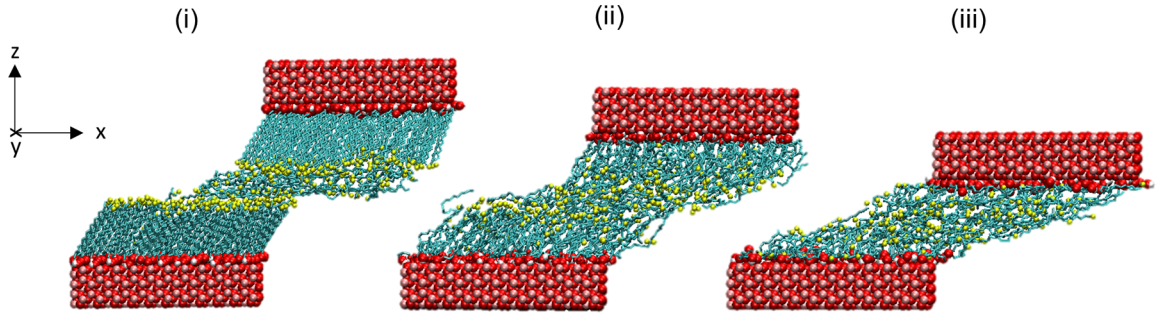


Figure 3. Simulation snapshots of representative OFM (SA) after 500 ps of sliding at high coverage (i), medium coverage (ii), and low coverage (iii), with P_z = 0.5 GPa and v_s = 10 m s^{-1}. Oxygen atoms are shown in red; head group hydrogen atoms, in white; terminal carbon atoms, in yellow; the other tail group carbon atoms, in cyan; and iron atoms, in pink. Hydrogen atoms in the tail groups are omitted for clarity. Periodic images and boundaries are not shown. Rendered using VMD.[45]

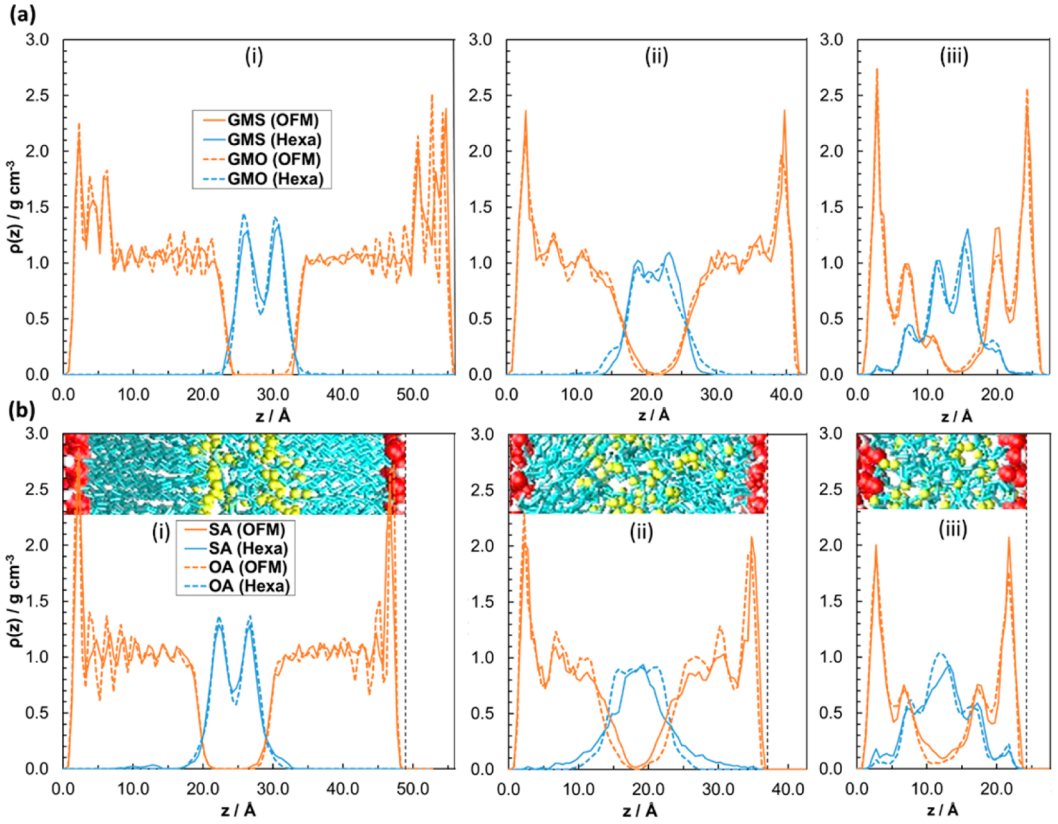


Figure 4. Atomic mass density profiles in z, $\rho(z)$, of OFM (orange) and hexadecane (blue) for (a) glyceride (GMS and GMO) and (b) carboxylic acid (SA and OA) head groups with stearyl (solid) and oleyl (dotted) tail groups at high (i), medium (ii), and low (iii) coverages. The vertical black dotted line in (b) shows the position of the top slab. Profiles for amides (SAm and OAm) as well as those under compression conditions are shown in the Supporting Information. Image overlay shows a section of the SA OFM film at corresponding coverages to help illustrate the interdigitation.

velocities.[48] At the onset of sliding, an expansion due to the increase in temperature by shear heating was expected, so it was ensured that steady-state sliding had been attained before sampling began for the friction coeffiecient.[36] The time taken to achieve steady-state sliding decreased with increasing sliding velocity but always equated to approximately 2 nm of sliding distance.

The kinetic friction coefficient, μ, was obtained using the extended Amontons−Coulomb law under the high load approximation:[16] $F_L/F_N = F_0/F_N + \mu \simeq \mu$. F_L and F_N are respectively the average total lateral and normal forces acting on each slab, and F_0 is the load-independent Derjaguin offset representing adhesive surface forces. The validity of this approximation was confirmed for two test cases (SA and GMO) by ensuring that a linear fit of F_L as a function of F_N gave an insignificant value of F_0 and the same result for μ within the statistical uncertainty. An insignificant value of F_0 was expected from previous simulations, which included a thin layer of lubricant confined between the monolayers.[15] In general, the assumption of $\mu \simeq F_L/F_N$ is appropriate for systems with low adhesion (small F_0) or under high applied loads (large F_N);[49] both of these are applicable to these simulations.

RESULTS AND DISCUSSION

The results are presented as follows. Results of the preliminary squeeze-out simulations are outlined first. This is followed by a detailed analysis of the structure of the film at different

DOI: 10.1021/acs.langmuir.6b00586
Langmuir XXXX, XXX, XXX−XXX

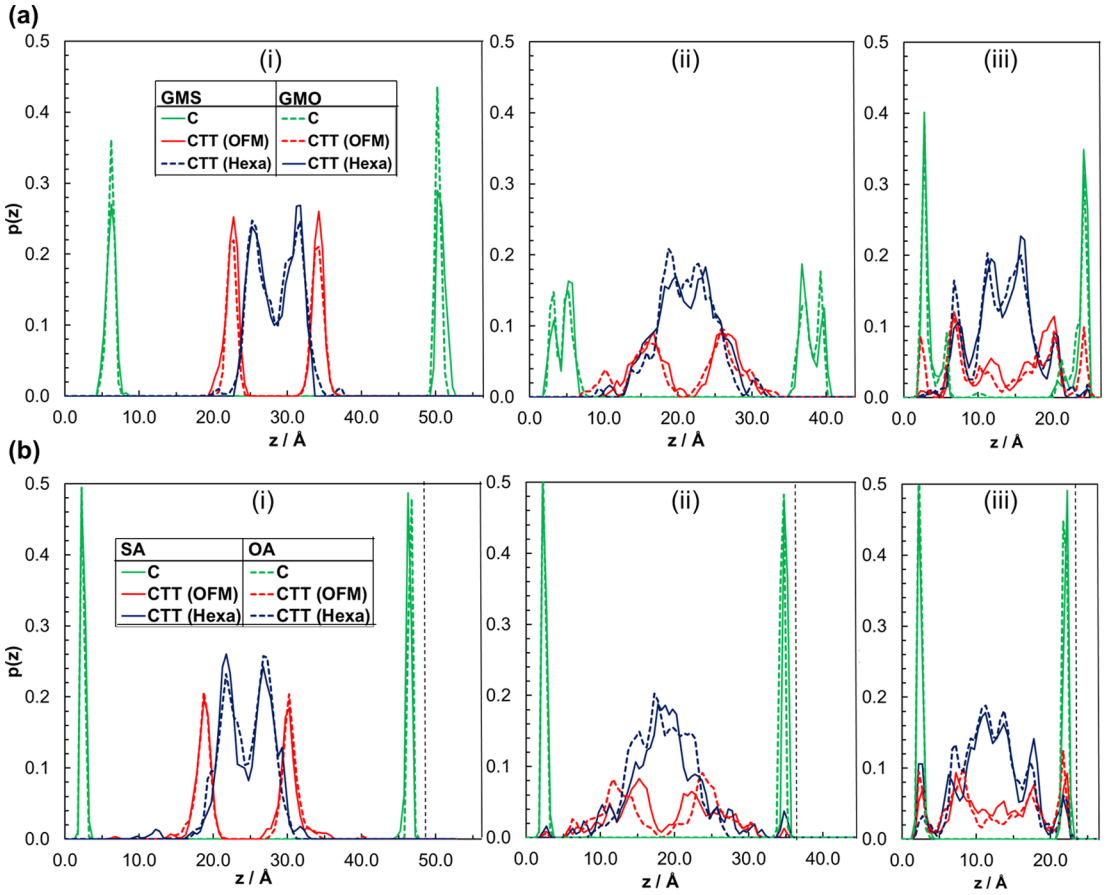


Figure 5. Atomic position probability profiles in z, $p(z)$, for carbonyl C (green), hexadecane terminal CTT (blue), and OFM terminal CTT (red) atoms in GMS and GMO (a) and SA and OA (b) at high (i), medium (ii), and low (iii) coverages. Profiles for other OFMs are shown in the Supporting Information. The vertical black dotted line in (b) shows the position of the top slab.

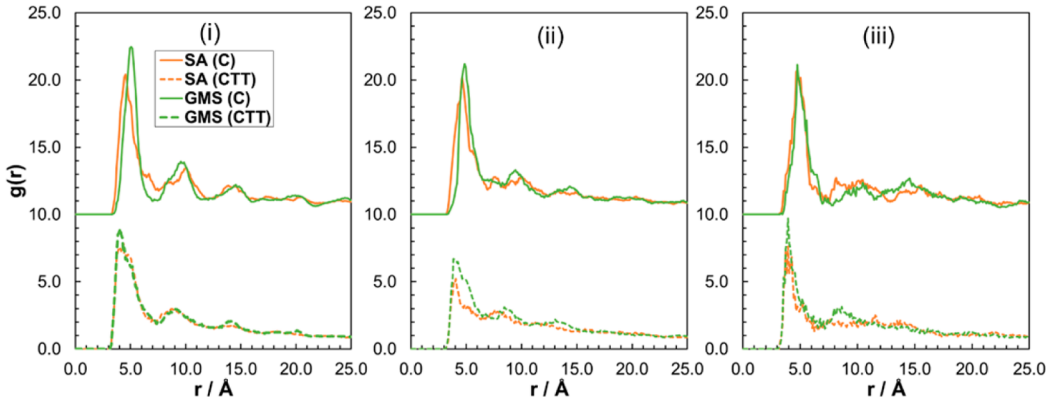


Figure 6. Radial distribution function (RDF) describing the ordering of the terminal CTT (dotted) and carbonyl C (solid) atoms for SA (orange) and GMS (green) at high (i), medium (ii), and low (iii) coverages. The C RDFs are shifted upward by 10 units for clarity.

coverages under sliding conditions. The friction results at different coverages and sliding velocities are then described and linked to the structural variations in the films. In what follows, some properties are expressed as functions of the distance from the surface, denoted by z; this is taken as the distance from the innermost layer of atoms on the bottom slab.

Preliminary Squeeze-Out Simulations. Simulations to establish the appropriate thickness of a boundary film of hexadecane under high pressure (P_z = 0.5 GPa) were performed first. The variation of the overall slab separation and of the number of confined hexadecane molecules from the beginning of the simulation is shown for a representative OFM (SA) in Figure 2. As expected, the slab separation distance (Figure 2a) decreases asymptotically to reach an equilibrium value.[41] Changes in gradient due to layer−layer transitions[41] are most easily observed at low coverage, where the deformation of the OFM has a less significant effect on the change in slab separation than at medium and high coverage. The equilibrium slab separation decreases from 30 Å at high coverage to 20 Å at low coverage. All of the OFM films deform considerably, leading to significantly thinner equilibrium slab separations than

DOI: 10.1021/acs.langmuir.6b00586
Langmuir XXXX, XXX, XXX−XXX

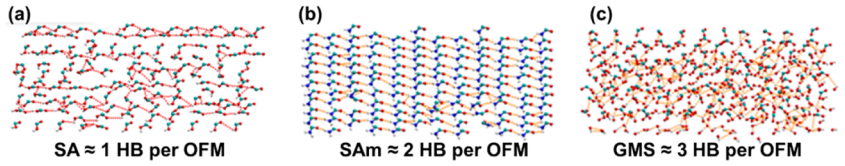


Figure 7. Snapshots of hydrogen bonding between OFM head groups at high coverage 500 ps into a sliding simulation: SA (a), SAm (b), and GMS (c). Head groups: oxygen shown in red; hydrogen, in white; nitrogen, in blue; and carbon, in cyan. Tail groups are omitted for clarity, and hydrogen bonds[52] are shown in orange.

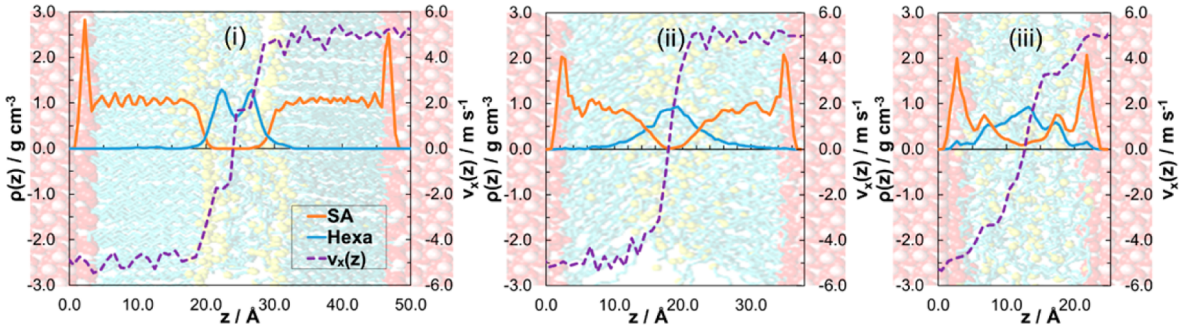


Figure 8. Profile of atom x velocities from 0.5 Å spatial bins in z, $v_x(z)$, overlaid on the mass density profile, $\rho(z)$, and a snapshot of representative OFM system (SA) at high (i), medium (ii), and low (iii) coverage. P_z = 0.5 GPa and v_s = 10 m s^{-1}.

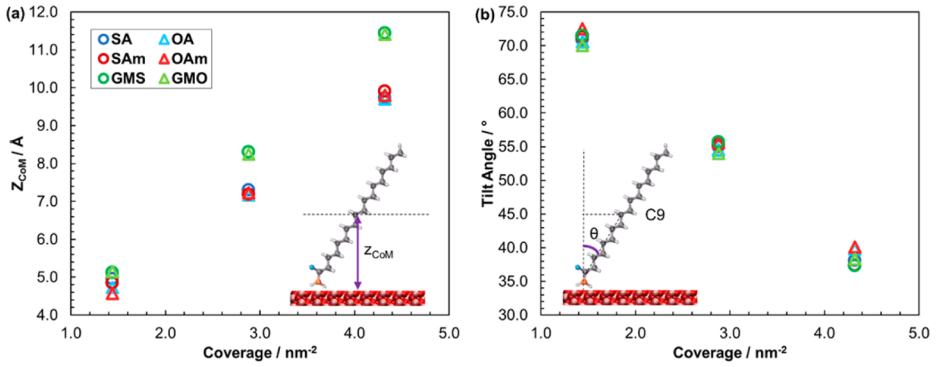


Figure 9. OFM film extension and orientation: average z_{CoM} of OFMs as a function of coverage (a), average C_{1-9} tilt angle as a function of coverage under sliding conditions (b), P_z = 0.5 GPa, v = 10 m s^{-1}. Error bars not shown as within the symbol size. Circles represent OFMs with saturated tail groups; triangles represent OFMs with tail group Z-unsaturation.

those found in subsequent compression and sliding simulations, where no vacuum is present in the x or y direction.

Figure 2b shows how the number of hexadecane molecules inside the contact volume decreases with time. Before 25 ps, there is little change in this value as the OFM film is compressed, but after this point, the number of molecules decreases asymptotically as expected.[41] The number of hexadecane molecules stabilizes at around 70 at all coverages, which corresponds to approximately two horizontally oriented molecular layers. Thus, these simulations suggest that the equilibrium number of hexadecane molecules remaining inside the contact volume is essentially independent of OFM coverage. This two-layer limit agrees well with extrapolations from previous squeeze-out simulations for C_3−C_{14} hydrocarbons between gold surfaces[40] as well as experimental AFM data for hexadecane between graphite surfaces, which suggest that the 2 → 1 layer transition occurs only above 0.6 GPa.[42] These results did not vary significantly between the different types of OFMs, so the subsequent compression and sliding simulations were based on systems containing 70 hexadecane lubricant molecules (2 molecular layers) for all types and coverages of OFM.

Structure during Sliding. Classical MD simulations of the OFM−hexadecane system under sliding conditions can yield important information regarding both the atomistic structure of the confined films and their friction behavior. Figure 3 shows simulation snapshots for a representative OFM (SA) at low, medium, and high surface coverages after 500 ps of sliding at 10 m s^{-1}.

The structure of the confined films has been studied under sliding conditions (v_s = 10 m s^{-1}) by analyzing their atomic mass density profile (Figure 4), atomic position probability profile (Figure 5), radial distribution function (Figure 6), hydrogen-bonding network (Figure 7), velocity profile (Figure 8), and center of mass and tilt angle (Figure 9). In general, the structure of the films remains very similar after the compression phase and during the sliding phase (Supporting Information), which is consistent with previous NEMD simulations.[16,21,50] However, the film structure changes significantly with OFM coverage and to a much lesser extent between different head groups and tail groups.

DOI: 10.1021/acs.langmuir.6b00586
Langmuir XXXX, XXX, XXX−XXX

The overall thickness and layering of the system in the z direction and the interdigitation of the OFM and hexadecane layers can be observed through mass density profiles, $\rho(z)$ (Figure 4), and atom position probability profiles, $p(z)$ (Figure 5). Data are shown for the saturated and unsaturated acids (SA and OA) and glycerides (GMS and GMO); amides (SAm and OAm) are an intermediate case between the two other head groups, so data for them are shown in the Supporting Information.

Sharp, intense peaks on the far-left and right-hand sides of Figure 4 indicate the adsorption of OFM head groups on the surface, and the less intense peaks which extend further from the surface are due to the tail groups. The OFM films become substantially thicker and more structured with increasing coverage. At high coverage (Γ = 4.32 nm^{-2}), the slabs are separated by approximately 50−55 Å, with up to 10 small peaks which indicate layering of the tail group carbon atoms. Comparing profiles from OFMs with stearyl (solid) and oleyl (dotted) tail groups, it is clear that the presence of Z unsaturation does not significantly alter the peak positions or slab separations. The high-coverage slab separations agree well with SFA experimental observations, which found that SA films on opposing mica surfaces in hexadecane (46−54 Å) were of similar thickness to those formed by OA (50−55 Å) when an elevated concentration of OA was used.[8] At medium coverage (Γ = 2.88 nm^{-2}), the slabs are separated by approximately 40 Å and the OFM tail groups show much less layering. At low coverage (Γ = 1.44 nm^{-2}), the slabs are separated by just 25 Å and the OFM displays only two clear peaks: a large peak at the surface incorporating both the head group and tail group atoms close to the surface and a smaller peak which extends to approximately 5 Å from the surface. The slab separation is greater for glycerides (Figure 4a) than for acids (Figure 4b) and amides as a result of the larger head group size, with the greatest difference being at high coverage (5 Å).

The height of the individual OFM films can be estimated by measuring the distance of the terminal carbon in the OFM tail, CTT, from the surface, as shown in Figure 5. At high surface coverage, glyceride film heights are approximately 21 Å (Figure 5a-i), whereas for acids (Figure 5b-i) and amides they are closer to 19 Å, which agrees well with experimentally measured film thicknesses from in situ AFM experiments.[13] At medium coverage, the average position of the OFM CTT peak is broader and shifted slightly closer to the surface (approximately 12 Å). At low surface coverage, there are two sharper OFM CTT peaks just 2 and 7 Å from the surface.

The intense carbonyl, C, peaks close to the surface in Figure 5 indicate that the head group positions are also localized in z. At low coverage, the C peaks are only 2 Å from the surface for all of the OFMs. For glyceride OFMs (Figure 5a), this suggests that most head groups are bound in a bidentate mode, with both alcohol groups bound to the surface. At medium coverage, the glyceride C profiles are significantly different from those for acids and amides, with a second peak of equal intensity appearing 5 Å from the surface. This suggests that, at medium coverage, around half of the molecules are bound in a bidentate mode with the C atoms close to the surface and half are bound in a monodentate mode with C atoms further from the surface. For high-coverage glyceride films, there is only a peak at 5 Å, suggesting that all molecules are now bound in a monodentate mode. The C peaks for acids (Figure 5b) and amides are generally far sharper than for glycerides (Figure 5a) due to the closer proximity of the C atoms to the surface.

Figures 4 and 5 also reveal important information regarding the level of interdigitation of the OFM films and the hexadecane lubricant, which is indicated by the penetration of the hexadecane profile into the OFM profile. The amount of penetration is influenced significantly by both the coverage and the head group type. For all of the OFMs tested, at high coverage two distinct hexadecane peaks form which correspond to well-separated layers. In Figures 4 and 5, the outer limits of the hexadecane peaks extend only to around 1 Å into the OFM peaks for glycerides (a-i), which increases to 3 Å for acids (b-i), indicating more interdigitation for the latter. At medium coverage, there is less layering of the lubricant, with only one broad hexadecane peak, the outer limits of which extend much further into the OFM film: 5 Å for glycerides (a-ii) and 10 Å for acids (b-ii). At low coverage, there is even more penetration of the hexadecane and OFM profiles, with a nonzero value for the OFMs in the center of the film, indicating that films on opposing slabs are directly interdigitated. In fact, at low coverage the hexadecane and OFM peaks directly overlap, suggesting that they form mixed layers which are likely to behave similarly to thin films of pure hexadecane.[51] The glyceride profiles at low coverage (a-iii) contain a larger number of better defined peaks than those for acids (b-iii) and amides (six vs five), suggesting more numerous well-separated layers.

The ordering within the OFM films was examined further by calculating separate radial distribution functions (RDFs), $g(r)$, for the head group carbon (C) and the terminal carbon (CTT). In Figure 6, the C RDFs are shifted upward by 10 units for clarity.

In Figure 6, the carbonyl carbon, C, shows long-range order for all OFMs and coverages, with the major peaks occurring at multiples of r = 5 Å. This corresponds to the unit-cell dimension of the hematite surface,[28] confirming that the surface dictates the head group packing in the OFM films.[16] Although the C peak at 5 Å is of similar intensity at all coverages, at high coverage, there are sharper peaks at 10, 15, and 20 Å, indicating increased long-range ordering and more solidlike films. At all coverages, the terminal CTT peaks are at least 25% less intense than the carbonyl C peaks, suggesting that the tail group positions are less ordered. However, at high coverage, there are still identifiable CTT peaks at 10, 15, and 20 Å, suggesting that the films remain solidlike at the interface between the OFM film and the hexadecane lubricant. At medium coverage, all of the CTT peaks are less sharp and intense than at high coverage, suggesting that the film is more amorphous with less correlation between the carbonyl and terminal carbon positions. At low coverage, the CTT peak at 5 Å is more intense than at medium coverage because the terminal carbon atoms are close enough to the surface such that it influences their packing. Overall, there appears to be a correlation between the intensity and long-range order of C and CTT peaks, suggesting that more ordered head group atoms can lead to more ordered tail group atoms. The peaks for GMS (Figure 6a) are generally sharper and more intense than those for SA (Figure 6b) at all coverages, suggesting that the former yields more ordered, solid-like films. OFMs with amide head groups represent an intermediate case between acid and glyceride head groups.

The differences in the phase of and level of interdigitation between films formed from different OFM head groups are postulated to be due to variations in the hydrogen-bonded networks, which are shown for the high -coverage case in Figure 7. These networks were analyzed in VMD[45] using

DOI: 10.1021/acs.langmuir.6b00586
Langmuir XXXX, XXX, XXX−XXX

standard criteria for hydrogen bonding,[52] i.e., a bond length cutoff of 3.9 Å and an angle cutoff of 90°. Intermolecular hydrogen bonding between the head groups appears to have an effect on the structure of the OFM-lubricant interface, through inducing a more solidlike film in glycerides than in acids. Amide OFMs are an intermediate case between acid and glyceride OFMs. Indeed, excluding those formed between the OFM and the surface, high-coverage GMS films contain approximately three intermolecular hydrogen bonds per molecule: SAm, two such bonds per molecule; and SA, one per molecule. The presence of unsaturation in the tail group has no effect on acid or amide OFMs; however, GMO forms only approximately two hydrogen bonds per molecule, perhaps explaining the greater levels of interdigitation in its films compared to those in GMS.

To understand flow within the confined films during sliding, velocity profiles, $v_x(z)$, for a representative OFM (SA) are shown in Figure 8. Velocity profiles are overlaid onto mass density profiles, $\rho(z)$, and a snapshot of the system in order to aid the interpretation of the results. Atom velocities are computed for 0.5 Å spatial bins which are averaged over 100 ps time blocks during the sliding phase. The velocity profiles at all coverages show that there is no slip at the surface, as expected for the strongly absorbed OFM head groups. The OFM tail groups move at a similar velocity as the slab to which they are absorbed ($\pm$5 m s^{-1}) until the region where they become interdigitated with the hexadecane lubricant. For SA at high coverage (i), these interfaces are at approximately 20 and 28 Å, at which points the gradient increases as the interface is sheared. At 22 and 26 Å, there is a flattening of the velocity profile, corresponding to the two hexadecane peaks in the mass density profile, with another increase in the velocity gradient at 24 Å between the two hexadecane layers. This suggests that these two hexadecane layers move as "plugs" between the OFM films, with three separate slip planes, i.e., at the OFM–hexadecane interfaces as well as between the two hexadecane layers. At medium coverage (ii), the slip plane becomes more difficult to define, and there appears to be significant shearing within the portion of the OFM tail group which is interdigitated with hexadecane. The velocity profile passes through zero at the center of the hexadecane layer, with a shallower gradient than at high coverage. The low-coverage velocity profile (iii) is more typical of conventional planar Couette flow, with a nearly linear velocity profile of the liquid between the slabs. However, the velocity profile still contains steps which indicate partial plug flow between combined OFM–hexadecane layers. Such stepped velocity profiles have also been observed in previous NEMD simulations of pure hexadecane films of similar thickness.[52]

The extension and orientation of the OFM films during sliding are further analyzed by calculating the average center of mass with respect to the z coordinate, z_{CoM} (Figure 9a) and also the tilt angle, θ, defined as the angle between a vector from the carbonyl C atom to the carbon atom halfway up the chain (C_9) and the surface normal (Figure 9b).

At low coverage, $z_{CoM} \approx 5$ Å and $\theta \approx 70°$, indicating that most molecules are lying almost flat on the surface. z_{CoM} increases linearly with coverage, at two different gradients depending on the head group. For acid (SA and OA) and amide (SAm and OAm) head groups, z_{CoM} reaches a maximum of approximately 10 Å at high coverage, and for glyceride head groups, the maximum is 11.5 Å as a result of the larger head group size. This means that, for the same tail group, glyceride OFMs yield slightly thicker films than acids or amides. OFMs with saturated and Z-unsaturated tail groups have similar z_{CoM} values, though saturated films are very slightly more extended (<0.2 Å). The tilt angle, θ, decreases linearly with coverage at the same rate for all of the OFMs, to approximately 55° at medium coverage and 40° at high coverage. The high-coverage value agrees reasonably well with tilt angles estimated from in situ AFM experiments, around 50° for SA[13] and stearyl amine[22] monolayers. Possible explanations for the 10° higher tilt angle in the experiments relative to these simulations include the fact that a higher pressure (1.6 GPa) was used in the experiments or that the experiments obtained a lower coverage than the highest used in these simulations. It is worth noting that both of these simulations and the in situ AFM experiments yield a significantly larger tilt than that observed in PNR experiments of stearyl amine on iron oxide surfaces under ambient conditions ($\theta \approx 22°$)[20] because of additional tilting under compression. In these simulations, θ appears to be independent of head group and tail group type, suggesting that once the molecules are subjected to high pressure (0.5 GPa), all of the molecules pack in a similar fashion regardless of head group type or tail group Z-unsaturation. This view is supported by previous high-pressure (0.3 GPa) simulations of close-packed alkanethiol monolayers on gold surfaces[44] which yielded a similar tilt angle ($\theta \approx 35°$); the slightly lower tilt angle can be rationalized through the lower applied pressure.

One might anticipate that θ would increase after sliding; however, under these simulation conditions (v_s = 10 m s^{-1}, P_z = 0.5 GPa), the average tilt angle remains very similar under both compression and sliding conditions. Rather than θ increasing, the tail groups rotate so that the molecular tilt aligns with the sliding direction, as can be observed from the average tilt orientation angle,[44] Φ, defined as the orientation of the tilt angle in the x–y plane, with 0° being completely aligned with the sliding direction (x). At the onset of sliding, $\Phi \approx 80°$ as the tilt is aligned predominantly perpendicular to the shear. After the sliding simulations at low and medium coverage, $\Phi \approx 20°$, indicating that the tilt almost completely aligns in the sliding direction. After the sliding simulations at high coverage, $\Phi \approx$ 40°, indicating partial alignment with the sliding direction, as has been noted in previous NEMD simulations of close-packed monolayers.[53] This partial alignment can be observed visually by comparing the snapshots shown in Figure 1 (compression) and Figure 3 (sliding). Longer simulations (10 ns) of high-coverage SA films at v_s = 10 m s^{-1} result in the same final tilt orientation angle ($\Phi \approx 40°$), suggesting that, under these conditions, the molecular tilt is unlikely to fully align with the sliding direction regardless of the sliding time. Previous NEMD simulations have suggested that at higher sliding velocities than those studied here (>30 m s^{-1}), the shear stress may be sufficient to pull molecules in high-coverage films into a completely aligned orientation.[44]

The fact that θ remains similar moving from compression to sliding conditions indicates that this angle is determined solely by the film response in supporting the applied pressure, whereas the applied sliding simply rotates the preferred tilt orientation toward the sliding direction. The partial alignment of the molecular tilt with the sliding direction does not have a significant effect on the friction coefficient, the 100 ps block average of which remains relatively constant throughout the course of the sampling period for all of the OFMs and coverages simulated (Supporting Information). Indeed, a simulation with the initial tilt aligned parallel to the sliding direction ($\Phi \approx 0°$) yielded a friction coefficient within the

DOI: 10.1021/acs.langmuir.6b00586
Langmuir XXXX, XXX, XXX–XXX

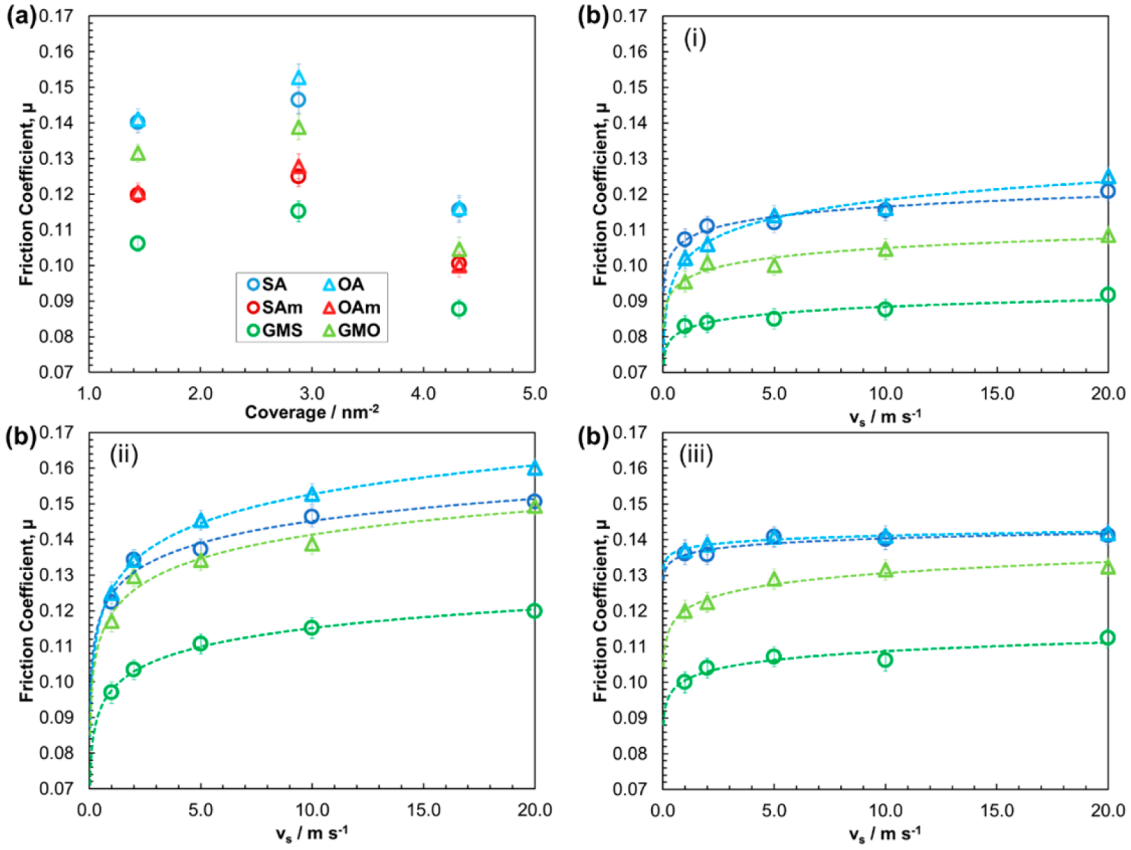


Figure 10. Friction coefficient: as a function of coverage at v_s = 10 m s^{-1} (a) and as a function of sliding velocity (b) at high coverage (i), medium coverage (ii), and low coverage (iii). The dotted line is a logarithmic fit of the friction−velocity data for each OFM. Error bars were calculated from the standard deviation between block averages from 100 ps time windows.

statistical uncertainty of that when the initial tilt was perpendicular to the sliding direction. Previous NEMD simulations of direct monolayer−monolayer[44] and monolayer−surface[53] systems showed an increase and decrease in friction, respectively, when the tilt was aligned with the sliding direction. The fact that friction appears to be independent of the orientation of the tilt angle in these NEMD simulations suggests that a thin lubricant layer between the OFM films is critical in maintaining the consistent low friction observed in previous NEMD simulations[15] and boundary friction experiments.[10]

Sliding Friction. The influence of surface coverage on the friction coefficient was probed at a sliding velocity of v_s = 10 m s^{-1} and a pressure of P_z = 0.5 GPa for acids, amides, and glycerides (Figure 10a). The variation in the friction coefficient with sliding velocity was also examined for acids and glycerides at a pressure P_z = 0.5 GPa (Figure 10b). The results indicate that the friction coefficient varies significantly with OFM coverage, head group type, and sliding velocity. Figure 10a shows that for all OFMs considered, at 10 m s^{-1} the friction coefficient at high coverage is around 30% lower than at medium coverage and approximately 25% less than at low coverage. On the basis of the structural information gathered at different coverages, this reduction in friction can be attributed to the formation of clear slip planes between the OFM films and the hexadecane lubricant, as observed through density (Figure 4), probability (Figure 5), and velocity profiles (Figure 8) as well as simulation snapshots (Figure 3). These slip planes are facilitated through the close-packing of the OFM tail groups, which leads to a solidlike, coherent monolayer film which allows very little interdigitation with the hexadecane lubricant or with each another. Indeed, large decreases in friction have also been observed for close-packed monolayers relative to loose-packed monolayers in previous NEMD simulations[24,54] and AFM experiments,[7,55] supporting the postulate that the formation of close-packed monolayers is important for the effective friction reduction of OFMs.[10]

The performance of the OFMs with respect to friction reduction is as follows: OA ≈ SA < OAm ≈ SAm ≈ GMO < GMS. As with the variation in coverage, the differences in film structure can also be used to explain the relative performance of the various OFM molecules; however, the differences are more subtle. Contrary to some previous suggestions regarding the action of glycerides as friction modifiers,[56] these simulations suggest that glycerides are able to act independently as friction modifiers on steel surfaces rather than merely serving as a reservoir for the acid. This hypothesis is supported by high-frequency reciprocating rig (HFRR) experimental results on steel surfaces, which showed higher friction coefficients for the disubstituted and trisubstituted glyceride than for the monosubstituted variant,[2] suggesting that the molecule as a whole is responsible for reducing friction, rather than its hydrolysis products. In fact, GMS is the most effective additive in reducing friction at all coverages in these simulations, and this is consistent with the structural information in Figures 4 and 5, which indicates less interdigitation between the OFM film and hexadecane for glyceride compared to acid and amide as a result of increased intermolecular hydrogen bonding (Figure 7). At low coverage, the reduced friction coefficient for glycerides relative to that for acids and amides is probably

DOI: 10.1021/acs.langmuir.6b00586
Langmuir XXXX, XXX, XXX−XXX

primarily due to increased layering[51] of the OFM−hexadecane system rather than reduced interdigitation. These results agree with boundary friction experiments which have shown that amides[9] and glycerides[10] with saturated tail groups yield lower friction coefficients than do acids. However, a smaller benefit of glycerides and amides relative to acids has been observed experimentally rather than being found in these simulations. This is probably due to lower glyceride and amide binding energies relative to that of the acid, which lead to lower surface coverage at equivalent concentrations; this possibility will be investigated in future adsorption experiments and DFT calculations.

To probe the effect of sliding velocity, v_s, on the friction of the OFM films, simulations with v_s = 1, 2, 5, 10, and 20 m s^{-1} were also conducted, as shown in Figure 10b. The chosen sliding velocities lie at the upper end of the range of experimentally relevant values while still being computationally feasible and reliably thermostattable.[48] Because experimental boundary friction data on steel surfaces at different velocities are available in the literature only for acids and glycerides,[10] amides are not included in these comparisons. It is noteworthy that, other than the orientation of the tilt angle mentioned previously, the film structures remained essentially unchanged through the course of the simulations over the entire range of sliding velocities simulated.

It is clear from the fitting curves in Figure 10b that the friction coefficient increases linearly with the logarithm of the sliding velocity for all of the OFMs and coverages, in accord with experimental results[9,10] and stress-promoted thermal activation theory.[5] The observed increase in friction with sliding velocity can be rationalized in the following way; as two atoms approach in the interdigitated region, they experience a repulsive force. At low sliding velocities and/or high temperatures, the molecules can adjust their geometry by thermally induced translation, rotation, and conformational changes in order to avoid increasing the repulsive force as the surfaces move past one another.[49] At high sliding velocities and/or low temperatures, thermal molecular adjustment alone becomes too slow and must be increasingly augmented by shear-stress-promoted adjustments, so the shear stress and thus the friction coefficient increase with sliding velocity.[54] Stress-promoted thermal activation models such as this yield a linear relationship between the logarithm of sliding velocity and the friction coefficient.[5,10] At high coverage, the barriers to interfacial sliding are small because there is very little interdigitation of the OFM film and the hexadecane lubricant (Figure 4-i), leading to a low friction coefficient which is only weakly influenced by the sliding velocity (Figure 10b-i). This behavior mirrors that observed in SFA experiments on high-coverage monolayer films of other surfactants.[57] At medium coverage, the amorphous OFM monolayers are more interdigitated by the lubricant (Figure 4-ii) and molecular adjustment is relatively slow because molecules are closely spaced. This means that activation barriers are both higher and more numerous, leading to a high friction coefficient which varies significantly with sliding velocity (Figure 10b-ii). At low coverage, the film is more liquidlike, and although the films are even more interdigitated (Figure 4-iii), the widely spaced OFM molecules are relatively free to rearrange in order to reduce the barrier height regardless of the sliding velocity.[58] This means that low-coverage films display a high friction coefficient which is almost independent of the sliding velocity (Figure 10b-iii).

At high velocity (v_s = 10 m s^{-1}), the friction coefficient increases by around 5% for all OFMs between low and medium coverage (Figure 10a) before decreasing by 30% between medium and high coverage. This pattern has been observed in SFA experiments using monolayer films formed from other surfactants in which friction increased as the film moved from a liquidlike to an amorphous film and then decreased when a solidlike film was formed.[58] This is because, at high velocity, the closely spaced molecules in medium-coverage films have insufficient time to adjust their positions without augmenting the shear stress. At low velocity (v_s = 1 m s^{-1}), the friction coefficient at medium coverage decreases to a value in between those at low coverage and high coverage (Figure 10b). This is because the molecules in medium-coverage films now have sufficient time to adjust their positions without significantly increasing the shear stress. Boundary friction experiments are always carried out at relatively low velocity, explaining why a steady reduction in friction is observed in these experiments when the concentration of the OFM is increased.[3,12]

The effect of tail group unsaturation on friction has been a topic of interest in many experimental[7,8,10] and simulation studies[16,17] of OFMs. The current simulation results suggest that, at equal coverage, the structure (Figures 4 and 5) and friction (Figure 10) of acid and amide OFMs with Z-unsaturated tail groups are very similar to their saturated counterparts. Thus, experimentally observed differences between acid and amide OFMs with saturated and Z-unsaturated tail groups are likely to have arisen from differences in their level of adsorption and thus surface coverage at the tested concentration, rather than from nanoscale structural differences. Although the binding energy of the OFM is not expected to change upon moving from saturated to Z-unsaturated tail groups,[17] the kink in the chain results in a larger kinetic barrier for the formation of a high-coverage film due to steric effects.[19] Indeed, in situ AFM[13] experiments have shown that, unlike SA, OA does not form close-packed monolayers on mica surfaces at equal concentration. Similarly, SFA experiments on steel surfaces have indicated that OA is able form close-packed monolayers, but only when it is added at much higher concentrations than SA.[8] This suggests that, in boundary friction experiments,[10] OFMs with saturated tail groups are more likely to form high-coverage films whereas OFMs with Z-unsaturated tail groups probably form low-coverage films. In these simulations, one can observe a 25% reduction in the friction coefficient upon moving from low to high coverage (Figure 10a). This level of reduction agrees well with experimentally observed differences between the friction coefficients of Z-unsaturated and saturated acid OFMs.[10] Moreover, the experimental friction coefficient for OFMs with saturated tail groups increases linearly with the logarithm of sliding velocity whereas the friction remains almost constant for OFMs with Z-unsaturated tail groups.[10] This friction−velocity behavior is also replicated in these simulations, with the friction of high-coverage (saturated) films increasing linearly with the logarithm of sliding velocity (Figure 10b) and low-coverage (Z-unsaturated) films displaying a friction coefficient which has only a very weak dependence on sliding velocity (Figure 10d). The simulations still show a very slight increase for low-coverage films as opposed to complete invariance observed experimentally. This difference can be explained through the possibility of a small amount of lubricant entrainment in the higher boundary friction experiment

DOI: 10.1021/acs.langmuir.6b00586
Langmuir XXXX, XXX, XXX−XXX

velocities,[9] which, at low coverage, may be sufficient to cancel the slight increase observed in these simulations.

The influence of the tail group Z-unsaturation on glyceride OFMs is different from that for acids and amides; specifically, saturated GMS is significantly (10%) more effective at reducing friction than Z-unsaturated GMO at all coverages and sliding velocities. This is mirrored by the fact that GMS films are less interdigitated by hexadecane, as shown in Figures 5a and 6a. The cause of these differences in structure and friction is postulated to be a disruption of the hydrogen-bonding network due to the kink in the tail group.

SUMMARY AND CONCLUSIONS

In this study, classical MD simulations with an all-atom force field have been used to investigate the structure and friction of films consisting of a range of model (SA and OA) and commercially relevant (SAm, OAm, GMS, and GMO) OFMs adsorbed on iron oxide surfaces and lubricated by a thin layer of hexadecane. The primary aim was to determine the effects of surface coverage and sliding velocity as well as head group and tail group type on the properties of interest. We have shown that NEMD simulations with accurate all-atom force fields are capable of describing the structure and friction of a complex multicomponent system when care is taken in the simulation setup. Indeed, we have found very good agreement between our results for aspects of the film structure and friction and experimental results reported in the literature.

Preliminary squeeze-out simulations demonstrate that, even at low coverage, OFM films are able to support a thin hexadecane film and prevent solid−solid contact at high pressure (P_z = 0.5 GPa). As the coverage is increased, the equilibrium film thickness increases; however, the amount of lubricant trapped in this film remains constant regardless of coverage and corresponds to two molecular layers of hexadecane. This thin layer of hexadecane appears to be critical in maintaining consistent low friction between high-coverage films.

Compression simulations indicate that the OFM molecules tilt under the applied pressure (P_z = 0.5 GPa) to an extent that depends on the coverage. At low coverage, the average tilt angle was 70°, but this dropped to 40° at high coverage. The latter angle and the high-coverage slab separation (50−55 Å) agree well with the experimental results. When sliding is applied, the average tilt angle does not change significantly, but the orientation of the tilt changes from being aligned perpendicular to predominantly, though not wholly, parallel with the sliding direction.

The simulations demonstrate the key role of OFM coverage in film structure and thus in boundary friction. At low coverage, the hexadecane molecules penetrate the OFM monolayers, leading to a loosely ordered film that responds under shear in a viscous, almost Couette-like fashion. By contrast, at high coverage the OFM monolayers form ordered, solidlike structures with negligible interdigitation between their methyl groups and the separating hexadecane layer. In these high-coverage films, shear is accommodated by slip planes between the well-defined OFM−hexadecane and hexadecane−hexadecane layers. Consequently, the friction coefficient is considerably lower at high coverage than at low coverage. The medium-coverage case gives an amorphous film structure which, at v_s = 10 m s^{-1}, leads to the highest friction of the three studied because it lacks both the fluidity of the low-coverage case and the clear slip plane formation that occurs at high coverage.

Amide and particularly glyceride OFMs yield lower friction coefficients than acid OFMs at all coverages in these simulations, as has been observed experimentally. This is achieved through the formation of intermolecular hydrogen bonds between proximal head groups, which results in more coherent films, thus allowing less lubricant interdigitation. These simulations suggest that glyceride OFMs are effective at reducing friction in their own right, and thus hydrolysis to the carboxylic acid may not be required in order to reduce boundary friction, as is sometimes proposed.

A linear increase in the friction coefficient with the logarithm of the sliding velocity is confirmed for all of the OFMs at all coverages, although the dependence is greatest for medium-coverage (amorphous) monolayers and very slight for low-coverage (liquidlike) monolayers. The results of the simulations suggest that differences in friction between high -coverage (solidlike) and medium-coverage (amorphous) OFM films will be relatively small under experimentally relevant boundary sliding velocities, whereas a 25% reduction is predicted when moving from low coverage to high coverage, as has been observed experimentally.

The simulation results provide strong evidence to suggest that the experimentally observed benefits of OFMs with saturated tail groups over those containing Z-unsaturation originate not primarily from the inherent structures of their films but rather from the ability to form films with a higher surface coverage. As a result, saturated OFMs should be used where possible to facilitate the formation of close-packed monolayers and maximize friction reduction in the boundary regime.

ASSOCIATED CONTENT

Supporting Information

The Supporting Information is available free of charge on the ACS Publications website at DOI: 10.1021/acs.langmuir.6b00586.

Full details of the nonbonded force-field parameters as well as additional structure and friction figures (PDF)

AUTHOR INFORMATION

Corresponding Author

*E-mail: j.ewen14@imperial.ac.uk.

Notes

The authors declare no competing financial interest.

ACKNOWLEDGMENTS

J.P.E. acknowledges the financial support of the Engineering and Physical Sciences Research Council (EPSRC) via a Case Conversion studentship and Shell Global Solutions via the University Technology Centre for Fuels and Lubricants at Imperial College London. H.A.S., C.G., and D.D. thank the EPSRC for support under Platform Grant EP/G026114/1. We also acknowledge the use of the Imperial College High Performance Computing Service for this research. URL: http://www.imperial.ac.uk/admin-services/ict/self-service/research-support/hpc/.

REFERENCES

(1) Spikes, H. Friction Modifier Additives. *Tribol. Lett.* **2015**, *60*, 5−5.

DOI: 10.1021/acs.langmuir.6b00586
Langmuir XXXX, XXX, XXX−XXX

(2) Davidson, J. E.; Hinchley, S. L.; Harris, S. G.; Parkin, A.; Parsons, S.; Tasker, P. A. Molecular dynamics simulations to aid the rational design of organic friction modifiers. *J. Mol. Graphics Modell.* **2006**, *25*, 495−506.
(3) Jahanmir, S.; Beltzer, M. An adsorption model for friction in boundary lubrication. *ASLE Trans.* **1986**, *29*, 423−430.
(4) Beltzer, M.; Jahanmir, S. Role of dispersion interactions between hydrocarbon chains in boundary lubrication. *ASLE Trans.* **1987**, *30*, 47−54.
(5) Briscoe, B. J.; Evans, D. C. B. The shear properties of Langmuir-Blodgett layers. *Proc. R. Soc. London, Ser. A* **1982**, *380*, 389.
(6) Jahanmir, S. Chain-length effects in boundary lubrication. *Wear* **1985**, *102*, 331−349.
(7) Ruths, M.; Lundgren, S.; Danerlov, K.; Persson, K. Friction of fatty acids in nanometer-sized contacts of different adhesive strength. *Langmuir* **2008**, *24*, 1509−1516.
(8) Lundgren, S. M.; Ruths, M.; Danerlov, K.; Persson, K. Effects of unsaturation on film structure and friction of fatty acids in a model base oil. *J. Colloid Interface Sci.* **2008**, *326*, 530−536.
(9) Ingram, M.; Noles, J.; Watts, R.; Harris, S.; Spikes, H. A. Frictional Properties of Automatic Transmission Fluids: Part I-Measurement of Friction-Sliding Speed Behavior. *Tribol. Trans.* **2010**, *54*, 145−153.
(10) Campen, S.; Green, J.; Lamb, G.; Atkinson, D.; Spikes, H. On the Increase in Boundary Friction with Sliding Speed. *Tribol. Lett.* **2012**, *48*, 237−248.
(11) Campana, M.; Teichert, A.; Clarke, S.; Steitz, R.; Webster, J. R. P.; Zarbakhsh, A. Surfactant Adsorption at the Metal-Oil Interface. *Langmuir* **2011**, *27*, 6085−6090.
(12) Simic, R.; Kalin, M. Comparison of Alcohol and Fatty Acid Adsorption on Hydrogenated DLC Coatings Studied by AFM and Tribological Tests. *Stroj. Vestn.-J. Mech. E* **2013**, *59*, 707−718.
(13) Campen, S.; Green, J. H.; Lamb, G. D.; Spikes, H. A. In Situ Study of Model Organic Friction Modifiers Using Liquid Cell AFM; Saturated and Mono-unsaturated Carboxylic Acids. *Tribol. Lett.* **2015**, *57*, 20.
(14) Luo, H.; Fan, W. Y.; Li, Y.; Zhao, P. H.; Nan, G. Z. Experimental and Molecular Dynamics Simulations for Investigating the Effect of Fatty Acid and Its Derivatives on Low Sulfur Diesel Lubricity. *China Pet. Process. Petrochem. Technol.* **2013**, *15*, 79−85.
(15) Eder, S. J.; Vernes, A.; Betz, G. On the Derjaguin Offset in Boundary-Lubricated Nanotribological Systems. *Langmuir* **2013**, *29*, 13760−13772.
(16) Doig, M.; Warrens, C. P.; Camp, P. J. Structure and Friction of Stearic Acid and Oleic Acid Films Adsorbed on Iron Oxide Surfaces in Squalane. *Langmuir* **2014**, *30*, 186−195.
(17) Loehle, S.; Matta, C.; Minfray, C.; Le Mogne, T.; Martin, J. M.; Iovine, R.; Obara, Y.; Miura, R.; Miyamoto, A. Mixed Lubrication with C18 Fatty Acids: Effect of Unsaturation. *Tribol. Lett.* **2014**, *53*, 319−328.
(18) Loehle, S.; Matta, C.; Minfray, C.; Le Mogne, T.; Iovine, R.; Obara, Y.; Miyamoto, A.; Martin, J. M. Mixed lubrication of steel by C18 fatty acids revisited. Part I: Toward the formation of carboxylate. *Tribol. Int.* **2015**, *82*, 218−227.
(19) Loehle, S.; Matta, C.; Minfray, C.; Le Mogne, T.; Iovine, R.; Obara, Y.; Miyamoto, A.; Martin, J. M. Mixed lubrication of steel by C18 fatty acids revisited. Part II: Influence of some key parameters. *Tribol. Int.* **2016**, *94*, 207−216.
(20) Wood, M. H.; Welbourn, R. J. L.; Charlton, T.; Zarbakhsh, A.; Casford, M. T.; Clarke, S. M. Hexadecylamine Adsorption at the Iron Oxide-Oil Interface. *Langmuir* **2013**, *29*, 13735−13742.
(21) Doig, M.; Camp, P. J. The structures of hexadecylamine films adsorbed on iron-oxide surfaces in dodecane and hexadecane. *Phys. Chem. Chem. Phys.* **2015**, *17*, 5248−5255.
(22) Campen, S.; Green, J. H.; Lamb, G. D.; Spikes, H. A. In Situ Study of Model Organic Friction Modifiers Using Liquid Cell AFM: Self-Assembly of Octadecylamine. *Tribol. Lett.* **2015**, *58*, 39−39.
(23) Casford, M. T. L.; Davies, P. B. The Structure of Oleamide Films at the Aluminum/Oil Interface and Aluminum/Air Interface Studied by Sum Frequency Generation (SFG) Vibrational Spectroscopy and Reflection Absorption Infrared Spectroscopy (RAIRS). *ACS Appl. Mater. Interfaces* **2009**, *1*, 1672−1681.
(24) Chandross, M.; Webb, E. B.; Stevens, M. J.; Grest, G. S.; Garofalini, S. H. Systematic study of the effect of disorder on nanotribology of self-assembled monolayers. *Phys. Rev. Lett.* **2004**, *93*, DOI: 10.1103/PhysRevLett.93.166103.
(25) Pastewka, L.; Moser, S.; Moseler, M. Atomistic Insights into the Running-in, Lubrication, and Failure of Hydrogenated Diamond-Like Carbon Coatings. *Tribol. Lett.* **2010**, *39*, 49−61.
(26) Li, Q. Y.; Dong, Y. L.; Perez, D.; Martini, A.; Carpick, R. W. Speed Dependence of Atomic Stick-Slip Friction in Optimally Matched Experiments and Molecular Dynamics Simulations. *Phys. Rev. Lett.* **2011**, *106*, DOI: 10.1103/PhysRevLett.106.126101.
(27) Plimpton, S. Fast parallel algorithms for short-range molecular-dynamics. *J. Comput. Phys.* **1995**, *117*, 1−19.
(28) Maslen, E. N.; Streltsov, V. A.; Streltsova, N. R.; Ishizawa, N. Synchrotron X-ray study of the electron-density in alpha-Fe2O3. *Acta Crystallogr., Sect. B: Struct. Sci.* **1994**, *50*, 435−441.
(29) Ramachandran, S.; Tsai, B. L.; Blanco, M.; Chen, H.; Tang, Y. C.; Goddard, W. A. Self-assembled monolayer mechanism for corrosion inhibition of iron by imidazolines. *Langmuir* **1996**, *12*, 6419−6428.
(30) Kawaguchi, M.; Yamamoto, M.; Nakamura, T.; Yamashita, M.; Kato, T. Surface properties of mono-, di-, and triglycerol monostearate monolayers spread at the air-water interface. *Langmuir* **2001**, *17*, 4677−4680.
(31) Jorgensen, W. L.; Maxwell, D. S.; TiradoRives, J. Development and testing of the OPLS all-atom force field on conformational energetics and properties of organic liquids. *J. Am. Chem. Soc.* **1996**, *118*, 11225−11236.
(32) Price, M. L. P.; Ostrovsky, D.; Jorgensen, W. L. Gas-phase and liquid-state properties of esters, nitriles, and nitro compounds with the OPLS-AA force field. *J. Comput. Chem.* **2001**, *22*, 1340−1352.
(33) Siu, S. W. I.; Pluhackova, K.; Bockmann, R. A. Optimization of the OPLS-AA Force Field for Long Hydrocarbons. *J. Chem. Theory Comput.* **2012**, *8*, 1459−1470.
(34) Murzyn, K.; Bratek, M.; Pasenkiewicz-Gierula, M. Refined OPLS All-Atom Force Field Parameters for n-Pentadecane, Methyl Acetate, and Dimethyl Phosphate. *J. Phys. Chem. B* **2013**, *117*, 16388−16396.
(35) Yeh, I. C.; Berkowitz, M. L. Ewald summation for systems with slab geometry. *J. Chem. Phys.* **1999**, *111*, 3155−3162.
(36) Berro, H.; Fillot, N.; Vergne, P. Molecular dynamics simulation of surface energy and ZDDP effects on friction in nano-scale lubricated contacts. *Tribol. Int.* **2010**, *43*, 1811−1822.
(37) Ryckaert, J. P.; Ciccotti, G.; Berendsen, H. J. C. Numerical-integration of Cartesian equations of motion of a system with constraints - molecular-dynamics of n-alkanes. *J. Comput. Phys.* **1977**, *23*, 327−341.
(38) Schneider, T.; Stoll, E. Molecular-dynamics study of a three-dimensional one-component model for distortive phase-transitions. *Phys. Rev. B: Condens. Matter Mater. Phys.* **1978**, *17*, 1302−1322.
(39) Gattinoni, C.; Mackowiak, S.; Heyes, D. M.; Branka, A. C.; Dini, D. Boundary-controlled barostats for slab geometries in molecular dynamics simulations. *Phys. Rev. E* **2014**, *90*, 13.
(40) Sivebaek, I. M.; Samoilov, V. N.; Persson, B. N. J. Squeezing molecular thin alkane lubrication films between curved solid surfaces with long-range elasticity: Layering transitions and wear. *J. Chem. Phys.* **2003**, *119*, 2314−2321.
(41) Persson, B. N. J.; Mugele, F. Squeeze-out and wear: fundamental principles and applications. *J. Phys.: Condens. Matter* **2004**, *16*, R295−R355.
(42) Gosvami, N. N.; Sinha, S. K.; Hofbauer, W.; O'Shea, S. J. Solvation and squeeze out of hexadecane on graphite. *J. Chem. Phys.* **2007**, *126*, 214708.
(43) Salacuse, J. J.; Denton, A. R.; Egelstaff, P. A. Finite-size effects in molecular dynamics simulations: Static structure factor and compres-

DOI: 10.1021/acs.langmuir.6b00586
Langmuir XXXX, XXX, XXX−XXX

sibility 0.1. Theoretical method. *Phys. Rev. E: Stat. Phys., Plasmas, Fluids, Relat. Interdiscip. Top.* **1996**, *53*, 2382−2389.
(44) Ramin, L.; Jabbarzadeh, A. Frictional properties of two alkanethiol self assembled monolayers in sliding contact: Odd-even effects. *J. Chem. Phys.* **2012**, *137*, 174706.
(45) Humphrey, W.; Dalke, A.; Schulten, K. VMD: Visual molecular dynamics. *J. Mol. Graphics* **1996**, *14*, 33−38.
(46) Liem, S. Y.; Brown, D.; Clarke, J. H. R. Investigation of the homogeneous-shear nonequilibrium-molecular-dynamics method. *Phys. Rev. A: At., Mol., Opt. Phys.* **1992**, *45*, 3706−3713.
(47) Bernardi, S.; Todd, B. D.; Searles, D. J. Thermostating highly confined fluids. *J. Chem. Phys.* **2010**, *132*, 244706.
(48) Toton, D.; Lorenz, C. D.; Rompotis, N.; Martsinovich, N.; Kantorovich, L. Temperature control in molecular dynamic simulations of non-equilibrium processes. *J. Phys.: Condens. Matter* **2010**, *22*, 074205.
(49) He, G.; Robbins, M. O. Simulations of the kinetic friction due to adsorbed surface layers. *Tribol. Lett.* **2001**, *10*, 7−14.
(50) Greenfield, M. L.; Ohtani, H. Packing of simulated friction modifier additives under confinement. *Langmuir* **2005**, *21*, 7568−7578.
(51) Savio, D.; Fillot, N.; Vergne, P. A Molecular Dynamics Study of the Transition from Ultra-Thin Film Lubrication Toward Local Film Breakdown. *Tribol. Lett.* **2013**, *50*, 207−220.
(52) McDonald, I. K.; Thornton, J. M. Satisfying hydrogen-bonding potential in proteins. *J. Mol. Biol.* **1994**, *238*, 777−793.
(53) Mikulski, P. T.; Gao, G.; Chateauneuf, G. M.; Harrison, J. A. Contact forces at the sliding interface: Mixed versus pure model alkane monolayers. *J. Chem. Phys.* **2005**, *122*, 024701.
(54) Kong, Y. C.; Tildesley, D. J.; Alejandre, J. The molecular dynamics simulation of boundary-layer lubrication. *Mol. Phys.* **1997**, *92*, 7−18.
(55) Lee, D. H.; Oh, T.; Cho, K. Combined effect of chain length and phase state on adhesion/friction behavior of self-assembled monolayers. *J. Phys. Chem. B* **2005**, *109*, 11301−11306.
(56) Tang, Z. L.; Li, S. H. A review of recent developments of friction modifiers for liquid lubricants (2007-present). *Curr. Opin. Solid State Mater. Sci.* **2014**, *18*, 119−139.
(57) Mazuyer, D.; Cayer-Barrioz, J.; Tonck, A.; Jarnias, F. Friction dynamics of confined weakly adhering boundary layers. *Langmuir* **2008**, *24*, 3857−3866.
(58) Yoshizawa, H.; Chen, Y. L.; Israelachvili, J. Fundamental mechanisms of interfacial friction: 1. relation between adhesion and friction. *J. Phys. Chem.* **1993**, *97*, 4128−4140.

DOI: 10.1021/acs.langmuir.6b00586
Langmuir XXXX, XXX, XXX−XXX